

MOA-cam3: a wide-field mosaic CCD camera for a gravitational microlensing survey in New Zealand

T. Sako ¹, T. Sekiguchi ¹, M. Sasaki ¹, K. Okajima ¹, F. Abe ¹, I. A. Bond ²,
J. B. Hearnshaw ³, Y. Itow ¹, K. Kamiya ¹, P. M. Kilmartin ³, K. Masuda ¹, Y. Matsubara ¹,
Y. Muraki ¹, N. J. Rattenbury ⁴, D. J. Sullivan ⁵, T. Sumi ¹, P. Tristram ³,
T. Yanagisawa ^{6,7} and P. C. M. Yock ⁸

1. Solar-Terrestrial Environment Laboratory, Nagoya University, Nagoya 464-8601, Japan
2. Institute for Information and Mathematical Sciences, Massey University, Auckland, New Zealand
3. Department of Physics and Astronomy, University of Canterbury, Christchurch, New Zealand
4. Jodrell Bank Observatory, The University of Manchester, Macclesfield, UK
5. School of Chemical and Physical Sciences, Victoria University, Wellington, New Zealand
6. Advanced Space Technology Research Group, Institute of Aerospace Technology, Japan Aerospace Exploration Agency(JAXA), Japan
7. Orbital Debris Program Office, National Aeronautics and Space Administration(NASA), USA
8. Department of Physics, University of Auckland, Auckland, New Zealand

Abstract

We have developed a wide-field mosaic CCD camera, MOA-cam3, mounted at the prime focus of the Microlensing Observations in Astrophysics (MOA) 1.8-m telescope. The camera consists of ten E2V CCD4482 chips, each having $2k \times 4k$ pixels, and covers a 2.2 deg^2 field of view with a single exposure. The optical system is well optimized to realize uniform image quality over this wide field. The chips are constantly cooled by a cryocooler at -80°C , at which temperature dark current noise is negligible for a typical 1-3 minute exposure. The CCD output charge is converted to a 16-bit digital signal by the GenIII system (Astronomical Research Cameras Inc.) and readout is within 25 seconds. Readout noise of 2–3 ADU (rms) is also negligible. We prepared a wide-band red filter for an effective microlensing survey and also Bessell V, I filters for standard astronomical studies. Microlensing studies have entered into a new era, which requires more statistics, and more rapid alerts to catch exotic light curves. Our new system is a powerful tool to realize both these requirements.

Keywords: CCD cameras, wide-field survey telescope, gravitational microlensing

1 Introduction

A decade after the first detection of gravitational microlensing events by the MACHO, EROS and OGLE groups [1][2][3], the study of microlensing has rapidly developed. The galactic dark matter problem which first motivated us is well summarized by the MACHO group [4]. They concluded MAssive Compact Halo Objects (MACHOs) consists of only 20% of galactic dark matter. However, with only 17 events, the statistics are not sufficient to make a definitive conclusion. Also the nature of MACHOs, where they exist and what they are, is not yet clearly understood.

To answer these fundamental questions, two new major survey projects have been started. One is OGLE-III [5] in Chile and the other is our project, MOA2, in New Zealand. Each group has a dedicated telescope and a wide-field camera to find more microlensing events. At the same time, the development of Difference Image Analysis (DIA) [6][7] enables us to make more rapid (almost in real time) event detections from huge quantities of image data.

Recently, extra-solar planet searches have become one of the main targets of microlensing studies. Contrasting with other planet searching techniques, the microlensing method is sensitive to Earth-size planets located within the habitable zone, even with current techniques [8]. This was at first thought to be difficult, because we must catch very small deviations from standard microlensing light curves. However, world-wide collaboration by survey teams (MOA, OGLE) with a rapid alert system (using DIA) and rapid follow-up teams (PLANET, μ FUN) have recently proved that this technique is really possible [9][10].

Our new project, MOA2, has finished the installation of the new 1.8-m MOA telescope at the end of 2004 at Mt John University Observatory in New Zealand. After pilot observations and tuning in 2005, we started a regular survey program and alert system in 2006. In this paper, we describe details of the wide-field camera mounted at the prime focus of

the new telescope. Details of the project and of the telescope will be presented elsewhere. We first describe the outline of the MOA project in Section-2 and details of the camera are explained in Section-3. The actual performance of the camera is presented in Section-3.7.

2 The MOA project (MOA and MOA2)

2.1 MOA

The MOA project [11] started in 1995 to search for microlensing events occurring in the Large Magellanic Cloud (LMC) and the Galactic Bulge (GB) directions. The team is a collaboration of Japan and New Zealand scientists. Observations are performed at Mt John Observatory in New Zealand (170.5°E, 44.0°S, 1029 m a.s.l.) using the 61-cm B&C telescope at the f/6.25 Cassegrain focus. At first, we started with a nine-CCD mosaic camera, MOA-cam1, each chip having 1k×1k pixels. In 1998, the camera was upgraded to MOA-cam2 which consists of three 2k×4k CCD SITe ST-002A chips. The details of MOA-cam2 are described by Yanagisawa et al. [12]

Mainly using MOA-cam2, MOA has successfully detected microlensing events [13], and also from the mass photometry database, MOA has studied variable stars [14][15]. MOA has also succeeded in establishing a rapid alert system for microlensing candidates [7][16]. This enables follow-up teams access to extensive photometry for the most interesting events.

2.2 MOA2

Following successful results from MOA1, MOA2 has been launched. MOA2 has its dedicated telescope specially designed for a wide-field microlensing survey. The mirror is 1.8 m in diameter and has a fast focal ratio value of f/3. Corrector lenses have been designed to realize good image quality over the wide focal plane at prime focus. The point spread caused by the optical

system is small enough over the entire focal plane, when compared with the typical seeing at Mt John. The combined optical system of primary mirror plus four corrector lenses results in an $f/2.91$ focal ratio and the available diameter of the focal plane corresponds to 2° .

MOA-cam3 is a specially designed camera installed at the prime focus of the MOA2 telescope. It is required that the wide focal area is covered by a well aligned mosaic of CCDs and a wide dynamic range to perform the photometry of millions of stars. These are crucial for the new microlensing survey programs.

The MOA2 telescope was constructed at the end of 2004. After pilot observations and tuning in 2005, regular observations have been performed since 2006.

3 MOA2 prime focus camera : MOA-cam3

3.1 Overview

As described in the previous section, the optical system makes a uniform image quality within a diameter of 2° at the focal plane. This area is covered by ten CCD chips aligned in a 5×2 array. The CCD chips are mounted on an aluminum-nitride ceramic plate (hereinafter AlN) and cooled down to -80°C (190 K) by a cryocooler through a copper braid. The clock, bias and output signals to/from the CCD are fed through hermetic Dsub connectors attached to the dewar wall. Electronic components are mounted just beside the dewar, so that even the longest signal cable becomes less than 90 cm. Communication from/to the host computer, placed in the adjacent observation room, is made through optical fibers.

All the components described above are packed into a compact volume as shown in Fig.1 and are mounted behind the corrector lenses, *i.e.*, at the prime focus. The camera is electrically insulated from the telescope body by a bakelite plate to avoid motor driver noise from the telescope. Also,

all the cables connected to the camera are electrically insulated from the telescope. A photo of the camera taken before mounting on the telescope is shown in Fig.2

In this section, we first introduce each component of the camera. The total performance is described in Section-3.7.

3.2 Dewar

The vacuum dewar is made of aluminum, except for the part of the bellows weld. The 8 mm thick top window is anti-reflection coated. (Here we define the 'top' as the direction from which the photons come.) Its transmissivity is more than 95% over a wide wave band, 400-950 nm.

Ten hermetic 37-pin Dsub connectors and one hermetic 40-pin round connector are attached on the side wall. Each Dsub connector corresponds to one CCD chip. The round connector is intended for multi-purpose use. This is actually used for monitoring the temperatures at the cryocooler cold head and the AlN plate. A heater is attached on the cooling path. Current for the heater can be fed through this connector when necessary.

The cryocooler cold head is also inserted in the vacuum space. To avoid the transfer of any vibration to the CCD chips, a bellows is placed between the main dewar and the cold head. The cryocooler is supported by four poles, which are connected to the heavy image rotator, that is a part of the telescope. Any cryocooler vibrations are damped out through these poles.

3.3 Vacuum and cooling system

A Gifford-McMahon cycle cryocooler GR-101 (AISIN SEIKI Co., Ltd.) is used to cool down the CCD chips. The weight of the cold head unit mounted on the camera is 5 kg. Compressed helium gas is fed through a 15-m flexible hose from a compressor located on the turn-table of the telescope. The cryocooler has 12 W cooling power and is connected to a 100 V/50 Hz power supply. A naive estimation of the heat injection to

the camera is about 11 W, which is almost all thermal radiation from the window and wall. (Details of the calculation method are found in [17].) Because we know this value is an overestimate for the real case, a cooling power of 12 W is deemed sufficient. The actual achievable temperature depends on the structure, such as the copper braid cross section, surface contact of each cooling component, vacuum level, outside temperature and so on. As the power of the cryocooler is not adjustable, we must operate it always at maximum power. The target is to achieve -80°C when the outside temperature is 10°C , which is the usual temperature during the summer nights at Mt John. Because we expect some level of over-cooling, a 3 W resistance heater is placed below the CCD mounting plate. By controlling the current in this resistance, we can keep a constant plate temperature.

The cold head of the cryocooler has its own vibrational motion during operation. The horizontal and the vertical oscillations of the cold head itself have been directly measured. These are shown in Fig.3. As shown in the figure, the vertical oscillation peak-to-valley amplitude is $14\text{ }\mu\text{m}$, which is less than the focal depth of $45\text{ }\mu\text{m}$. The horizontal oscillation peak-to-valley amplitude is $7\text{ }\mu\text{m}$, which corresponds to half a pixel size and also to 0.3 arcsec. This is almost negligible when compared with the typical seeing of 2.0 arcsec at Mt John. Furthermore, we must note that the cold head vibration does not directly transfer to the image plane, because the cold head is connected to the AlN plate via a copper braid.

The cooling power and the vacuum level are strongly correlated. When the vacuum level is worse (that is the pressure is higher), thermal conduction results in more heat input and the temperature rises. When the temperature becomes higher, molecules adsorbed on the cold components are released, and the pressure increases. Above a certain critical level, this positive feedback catastrophically increases the CCD temperature. In the case of our camera, the critical level was roughly around 10^{-3} mbar in pressure. So we tried to keep below this pressure after removing the dewar

from the vacuum pump. The pressure in the dewar and temperatures at the AlN and the cold-head are always monitored by a remote PC. Fig.4 shows long-term temperature and pressure profiles measured at Mt John in 2005 August. The curves show stable temperature and pressure profiles for a month. The AlN temperature is well maintained around our target temperature of -80°C . From the laboratory tests, we know that the thermal noise at -70°C is typically 1 ADU in 100 s, and it starts to increase when the temperature exceeds -60°C . We can see that our observations are all made below this limit. As no trend is found during a month, we don't expect to have to vacuum pump the dewar as frequently as every month. However, in the New Zealand summer time, we need pumping every few days to a week.

The diurnal variation of $\Delta T \sim 30\text{ K}$ causes a scale variation of AlN to be $24\text{ }\mu\text{m}$ (1.6 pixel or 0.93 arcsec) over the field of view (200 mm in diameter). Because our analysis is performed dividing the field into small subareas of $1\text{k} \times 1\text{k}$ pixels, the scale variation is reduced to be 0.1 pixel that can be compensated by DIA. Some investigations to keep the temperature more stable are now under progress. Improving the dome temperature control in summer time and driving the cryocooler with a higher frequency (60 Hz) should keep the temperature below -80°C all the time. Installing an ion pump may also be a promising way, but we must work within a limited volume at the prime focus. Once the camera is overcooled, we can control the temperature by using the heater installed in the camera so that we can keep a constant temperature.

As a reference, we also show two other profiles in Fig.5. These plots show the pressure evolution after removing the dewar from the pump. The only difference between the two plots is whether or not use molecular sieves in the dewar. In the actual setting, we attached 100 g of Molecular Sieves 5A 1/16 (WAKO) at the cold head, where it is usually cooled down to -150°C (120 K). Because the adsorption of the molecular sieves is more effective at low temperature, they are packed in a copper box with a copper mesh at

one surface.

3.4 CCD

MOA-cam3 uses ten E2V CCD4482 chips. Each chip has $2k \times 4k$ pixels and is a back-illuminated CCD. The pixel size is $15 \mu\text{m}$ square, which corresponds to 0.58 arcsec when combined with the $f/2.91$ optics. The cataloged sensitivity and the full dynamic range are $6.0 \mu\text{V}/\text{electron}$ and $150k\text{-}200k$ electrons, respectively. The quantum efficiency as a function of wavelength is shown in Fig.6.

We arranged 10 chips in a 5×2 array resulting in a $10k \times 8k$ mosaic camera for the total system. The gap between chips is set to be 0.5 mm . Because each chip has an insensitive area of 0.5 mm on both sides and 0.17 mm at the top (opposite to the readout side), the inter-chip inactive space becomes 1.5 mm and 0.84 mm , respectively. Excluding these inactive areas, the chips cover 2.18 deg^2 .

The chips must maintain a flatness of within $\pm 45 \mu\text{m}$, which results in one pixel size of defocussing. We prepared an AlN mother plate to mount the chips. Because the thermal expansion coefficient of AlN, $4.0 \times 10^{-6} \text{ K}^{-1}$, is very similar to that of the package of the chips, $1.2 \times 10^{-6} \text{ K}^{-1}$, which is made of invar, even a large temperature change of $\Delta T \sim 120 \text{ K}$, does not damage the chips. At the same time, the thermal conductivity of AlN, 170 W/m/K , is high, so that effective cooling can be realized. The flatness of the AlN plate is kept to within $\pm 10 \mu\text{m}$ (min-max). Also the flatness of each chip is guaranteed to be within $\pm 20 \mu\text{m}$ (min-max). After mounting the chips on the plate, we measured the flatness of the whole chip array. The relative depth of a total 832 points on the chips was measured using an automatic non-contact 3-dimensional measurement stage (NH-6, Mitaka Kohki Co., Ltd.) at Nagoya University. The result is shown in Fig.7 and Fig.8. As seen in the figure, the depth variation is within $25 \mu\text{m}$ (min-max). We can even find the surface structure of each chip. This is a satisfactory

result which conforms to the optical requirements of the telescope and detector system.

The AlN plate is supported on the dewar via four polycarbonate poles. Because the thermal conductivity of polycarbonate is 0.1 W/m/K , the expected heat injection from these supports is only 0.08 W , so that the conducted heat input is negligible.

Fig.9 is a photo of the CCD array mounted on the AlN plate and placed in the camera dewar.

3.5 Electronics

To drive an E2V CCD4482 chip, we need nine clock signals and five DC biases. To feed these signals to the chips, we used the GenIII system from Astronomical Research Cameras Inc. (hereinafter ARC). The system contains one timing board which communicates with the host computer via optical fiber cables and controls all the other boards. Two clock boards are used to provide clock signals to the chips. Each board sends an identical set of clock signals to five chips. Five video boards are used to feed DC biases, which are tuned for each chip. Each video board can generate 12 independent DC biases, and they are separated to two chips. A video board also has two 16-bit A/D converters to digitize the output signal from two chips. The A/D converters follow the amplifiers, and the correlated double-sampling method is used to pick-up the correct signal for each pixel.

The signal integration time, bias voltages, amplifier gain (it is selectable from 1, 2, 5, 10) are all consistently adjusted to match the chip and A/D dynamic ranges, which means that 200k electrons correspond to 2^{16} ADU ($3.1 \text{ e}^-/\text{ADU}$). The results of readout tuning are introduced in Section-3.7

The commands and clock pattern are recorded on the DSP chip on the timing board. Observers communicate with the timing board from the host computer, where a PCI board is installed. In our system, the host computer is operated under Linux OS, and the camera control commands

are implemented in the C language using the libraries provided by ARC.

3.6 Peripherals

The shutter and filters are also controlled from the camera control computer via RS232C. The host computer communicates with another computer to control the telescope and all the commands to the electronics, shutter, filters and telescope are synchronized.

The shutter is placed between the camera window and the last corrector lens element. The bidirectional roll-type shutter enables a uniform exposure over the wide image area. Filters are located in the space between the second and third of the four corrector lenses. They are usually parked parallel to the telescope axis, but turn perpendicular into the light path when in use. This system can reduce the light obscuration by the filters when parked. We prepared a wide-band red filter for an effective microlensing survey and also Bessell V, I filters for standard astronomical studies.

To avoid frosting on the camera window, nitrogen gas is introduced into the gap between the window and last lens. Because the space is well packed, only a slow flow of gas is sufficient.

3.7 Performance

After adjusting the DC bias voltages for each chip, we have measured the dynamic range and linearity using LED light. An example of LED calibration for one chip is shown in Figure-10. Figure-10 a) shows the mean ADU in a small 100×100 -pixel area as a function of the LED illumination time. The deviation from linearity is only 1% at maximum and is limited by the stability of the LED intensity. Figure-10 b) shows a relation between the mean and the variance of the ADU in the same small area. When the variance is dominated by photon statistics, we can expect a linear relation, as seen in the plot below 40 000 ADU. Here the slope gives the inverse of the AD conversion coefficient, the so-called gain. The

constant offset is determined by the readout noise that is measurable from a dark image with zero exposure. The chip-to-chip variation of the gain and the readout noise are $2.0\text{--}2.4\text{ e}^-/\text{ADU}$ and $5\text{--}7$ electrons ($2\text{--}3\text{ ADU}$) in rms, respectively. The gain values are smaller than the expected one introduced in Section-3.5 because the coarse gain of the GenIII amplifier could not be compensated. The measured readout noise is consistent with the cataloged value of GenIII. We also found electrical noise due to the telescope motor drivers and reduced it at the level of the readout noise. This was achieved by electrically insulating the camera and the telescope as described in Section-3.1 while the rearrangement of grounding did not work as effectively as insulation. Because the dark sky background level at Mt John in a 1-minute exposure is typically a few 1000 ADU/pixel , these electrical sources of noise are negligible. When the CCD saturates, the linearity breaks down, as is seen in Figure-10 b) at a mean ADU of $40\,000$. This effect is also visible as a distortion of the image. The breaking points are around $30\,000\text{--}40\,000\text{ ADU}$ in the 10 chips. Combining with the gain, the measured dynamic range (80k electrons in average) is half of the catalog value. We could not find better settings whilst keeping the gain variation of ten chips as small as possible.

To achieve the condition described above, we chose a readout speed of $3.1\text{ }\mu\text{s/pixel}$. Because the signal transfer is far faster than the A/D conversion, the readout to the host computer is done in serial for the 10 chips. Then the total readout for the 10 chips is completed in 25 seconds. These measurements and tunings were carried out both in the laboratory and after the camera was mounted on the telescope. Fig.11 shows an image of a part of the Large Magellanic Cloud taken by the new MOA telescope and MOA-cam3. The Tarantula nebula (30 Doradus; $\sim 0.4^\circ$ in diameter), seen in the right bottom corner, demonstrates the width of the field.

4 Summary

The mosaic CCD camera MOA-cam3 was constructed to be installed at the new 1.8 m MOA2 telescope prime focus. It consists of ten E2V CCD4482 chips, each having $2k \times 4k$ pixels. Combined with the $f/2.91$ optics, it covers 2.2 deg^2 in a single exposure. The chips are well aligned on the mother plate, with a satisfactory flatness of $25 \mu\text{m}$ peak-to-valley. The chips are cooled by a cryocooler to around -80°C , at which temperature the dark current of the chips is negligible during the typical exposure time of a few minutes. The chips are controlled from a Linux PC via the GenIII system. The gain and dynamic range of the chips are tuned by the DC bias voltage, and readout speed is set to match the 16-bit ADU and chip saturation level. The readout noise after tuning is 2–3 ADU in rms, which is negligible in relation to the sky background for a typical exposure. There is also noise due to the telescope drive. We reduced it to the level of the readout noise by electrically insulating the camera and telescope body. The host computer also controls the shutter and filters. By communicating with the telescope control PC, all the observations are automatically processed. Although MOA-cam3 is already in operation with sufficient power for a dedicated microlens survey program, some improvements described in this manuscript are also under progress to make it more general purpose instrument.

MOA2 started regular observations in 2006. Using a real time analysis technique, a rapid microlensing alert system has also been started. This is being upgraded to be yet more rapid and reliable in 2007. It means that the other follow-up teams have access to plenty of exotic microlensing events, which is vitally important in this new field of research. At the same time, our wide-field camera has an excellent capability for monitoring exotic microlensing events without the need for external alerts, as well as discovering serendipitous astronomical phenomena.

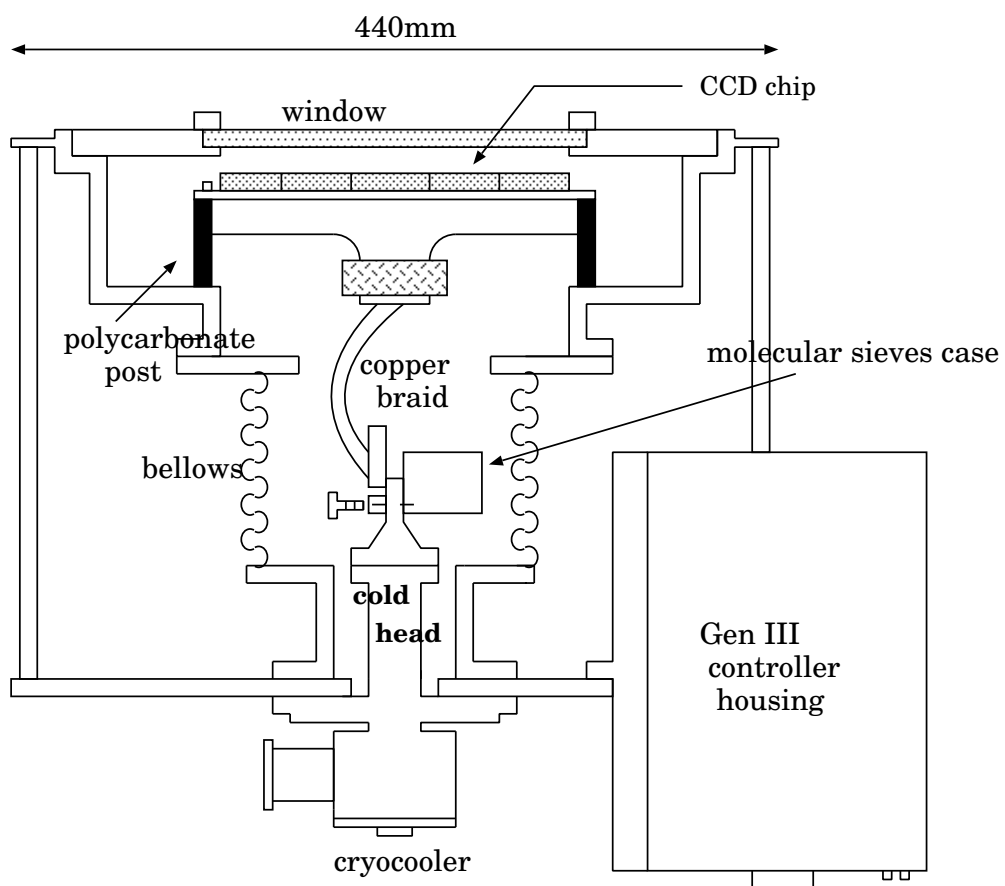
Acknowledgments

This work is supported by a grant-in-aid for scientific research of the Japan Ministry of Education, Science, Sports and Culture. The authors are grateful to the staff of the National Astronomical Observatory Japan (Y. Kobayashi, S. Miyazaki, Y. Komiyama, H. Nakaya), to members of the Graduate School of Science (S. Sato, H. Shibai) and Instrument Development Group of the Technical Center of Nagoya University, to J. Hiraga in ISAS/JAXA, to staff of the Nishimura Co. Ltd., to H. Kondoh in AISIN, to A. Rakich in IRL and to B. Leach in ARC. Finally the authors thank the anonymous reviewer to improving the manuscript and for general expert comments on the camera.

References

- [1] Alcock, C., et al., 1993, *Nature*, 365, 621
- [2] Aubourg, E., et al., 1993, *Nature*, 365, 623
- [3] Udalski, A., et al., 1993, *Acta. Astron.*, 43, 289
- [4] Alcock, C., et al., 2000, *ApJ*, 542, 281
- [5] Udalski, A., 2003, *Acta Astron.*, 53, 291
- [6] Alard, C. and Lupton, R. H., 1998, *ApJ*, 503, 325
- [7] Bond, I. A., 2001, *MNRAS*, 327, 868
- [8] Bennett, D. P. and Rhie, S. H., 1996, *ApJ*, 472, 660
- [9] Udalski, A., 2005, *ApJ*, 629, L109
- [10] Beaulieu, J.-P., 2006, *Nature*, 439, 437
- [11] Muraki et al., 1999, *Prog. of Theor. Phys. Suppl.*, 133, 233
- [12] Yanagisawa, T., et al., 2000, *Experimental Astronomy*, 10, 519

- [13] Sumi, T., et al., 2003, ApJ, 591, 204
- [14] Noda, S., et al., 2004, MNRAS, 348, 1120
- [15] Abe, F., et al., 2005, MNRAS, 364, 325
- [16] <http://www.massey.ac.nz/~iabond/alert/alert.html>
- [17] Miyazaki, S., et al., 2002, PASJ, 54, 833



[MOA-cam3 overview]

Figure 1: Schematic view of MOA-cam3.

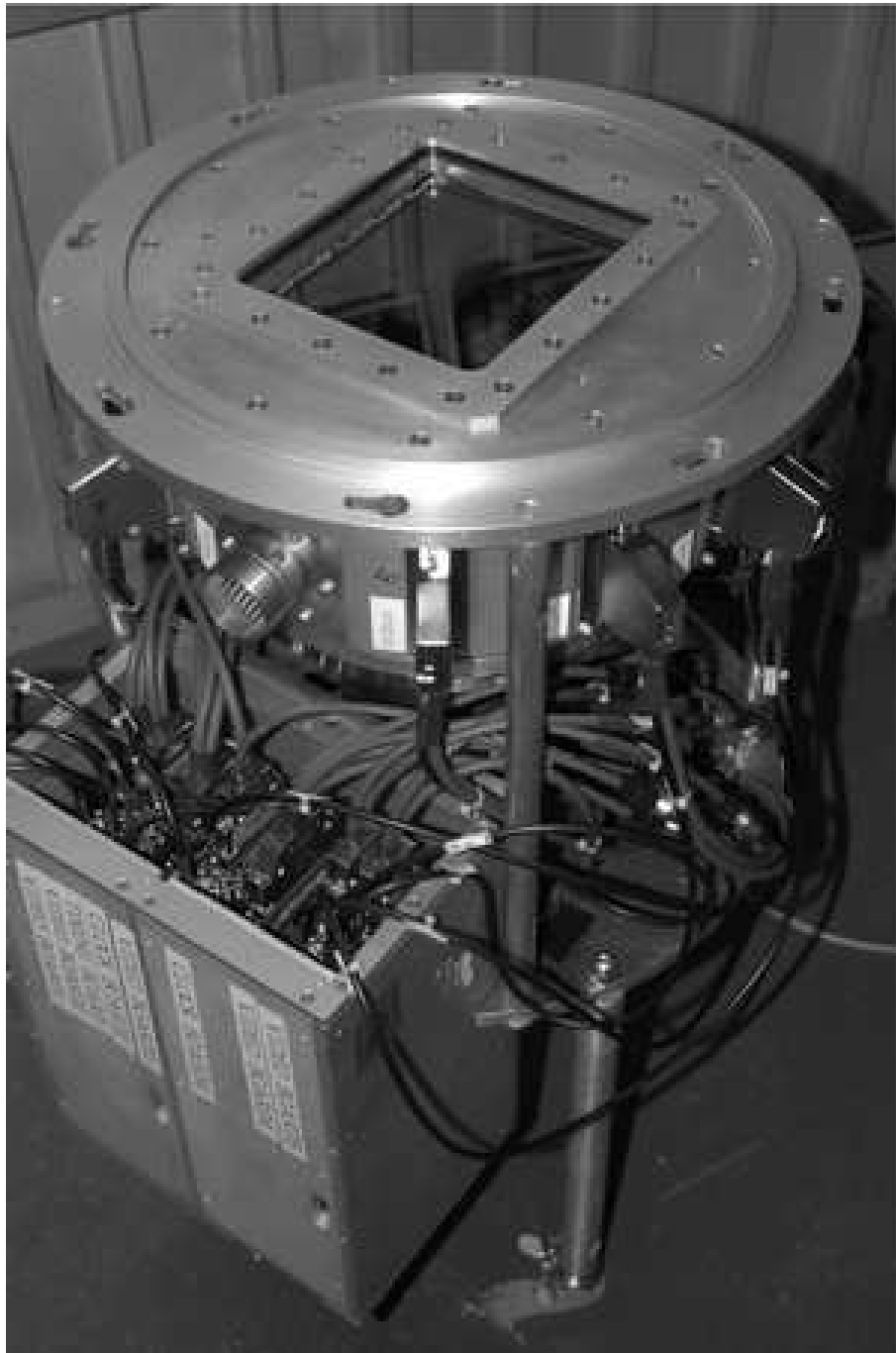


Figure 2: Photo of MOA-cam3.

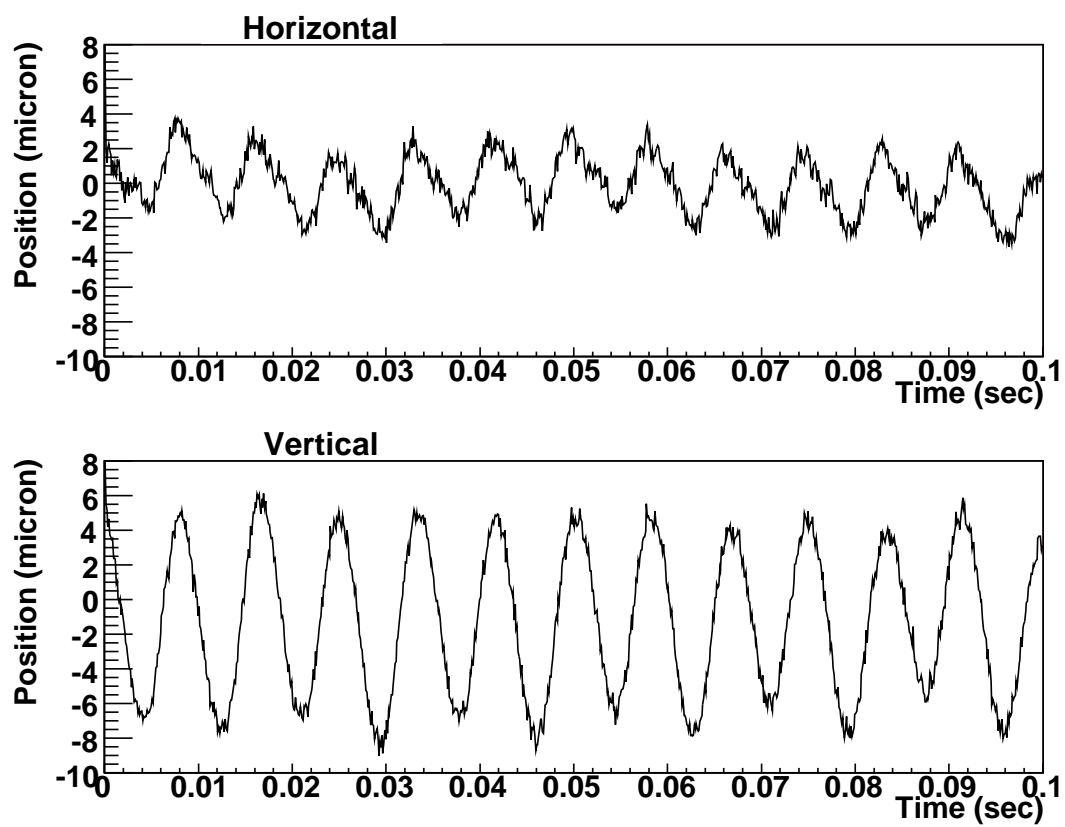


Figure 3: Vibration of the cryocooler cold head. Relative position of the cold head during its operation was measured in the horizontal and vertical directions.

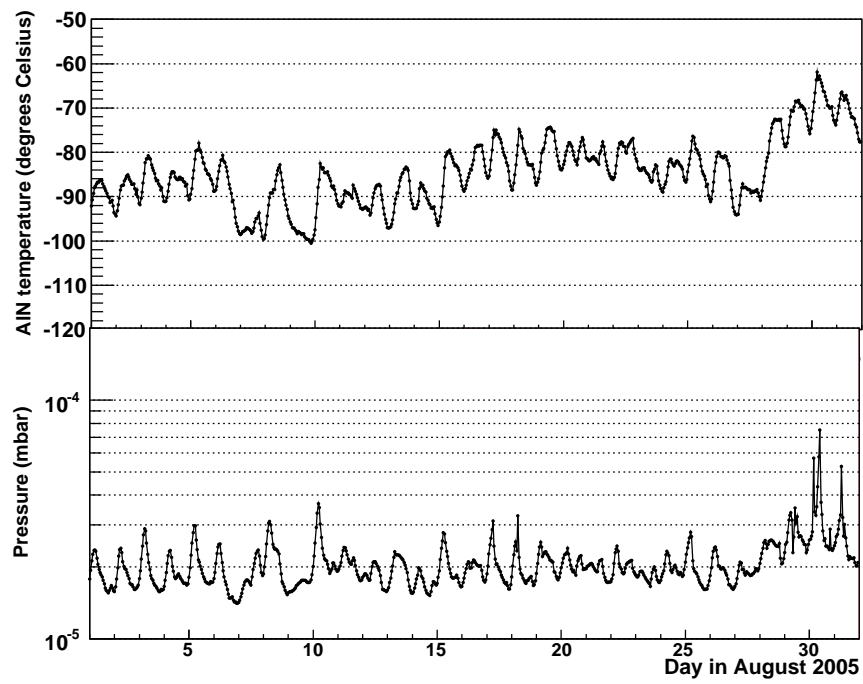


Figure 4: Long term profile of the inner dewar pressure and AIN temperature. Though daily variation correlating to the outside temperature is seen, AIN temperature is well kept around -80°C for one month.

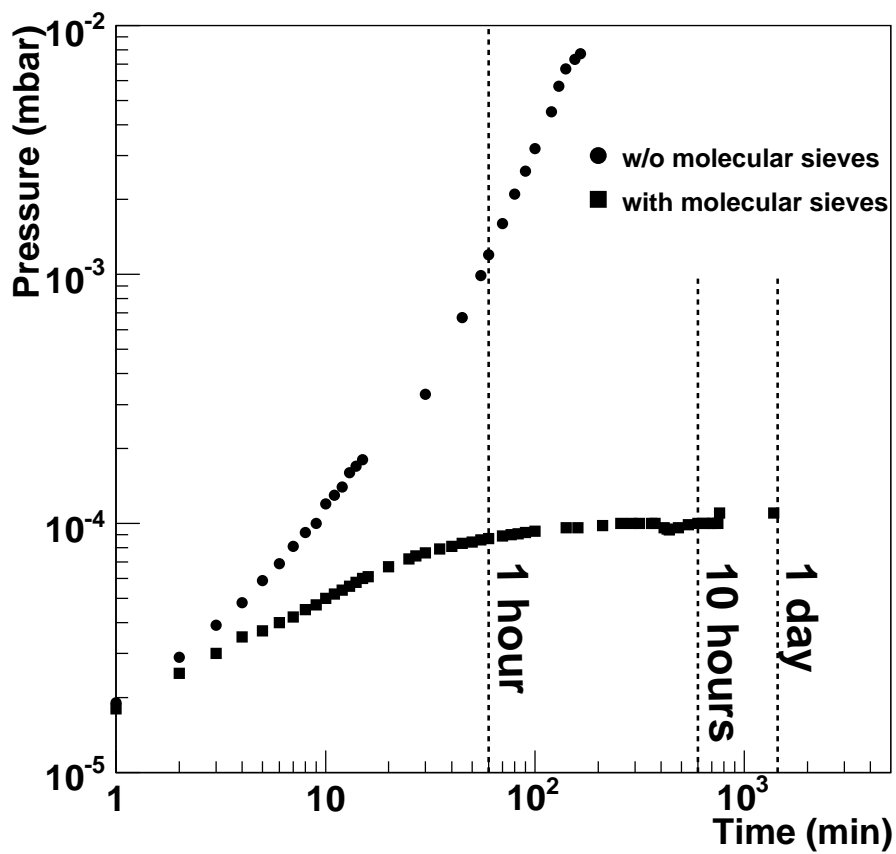


Figure 5: Time profiles of the dewar pressure with and without using molecular sieves. The start time is defined at the moment when the valve was closed after sufficient vacuum pumping. The circles and the squares indicate for the case of without/with the molecular sieves, respectively. The effect of the molecular sieves is apparent.

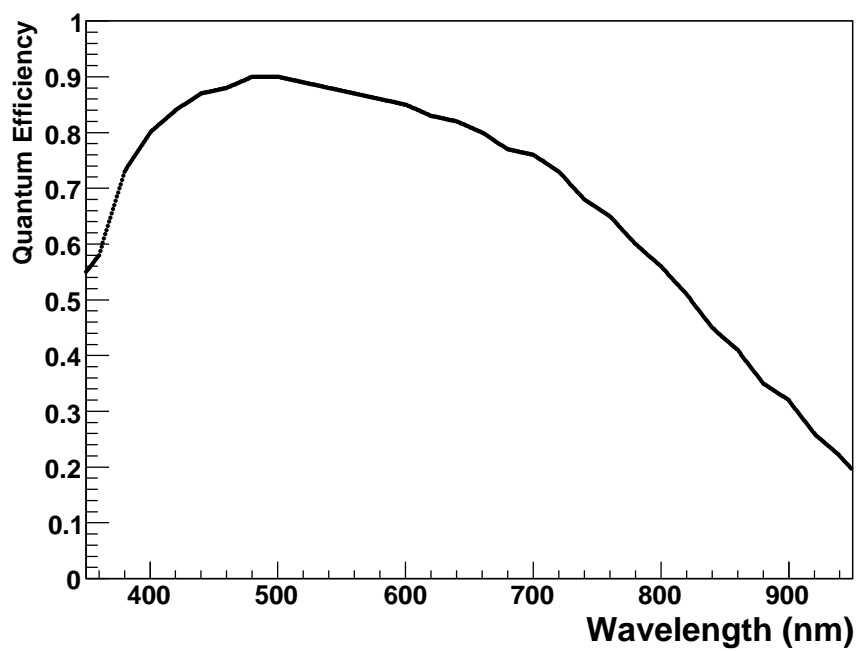


Figure 6: Quantum efficiency of E2V CCD4482.

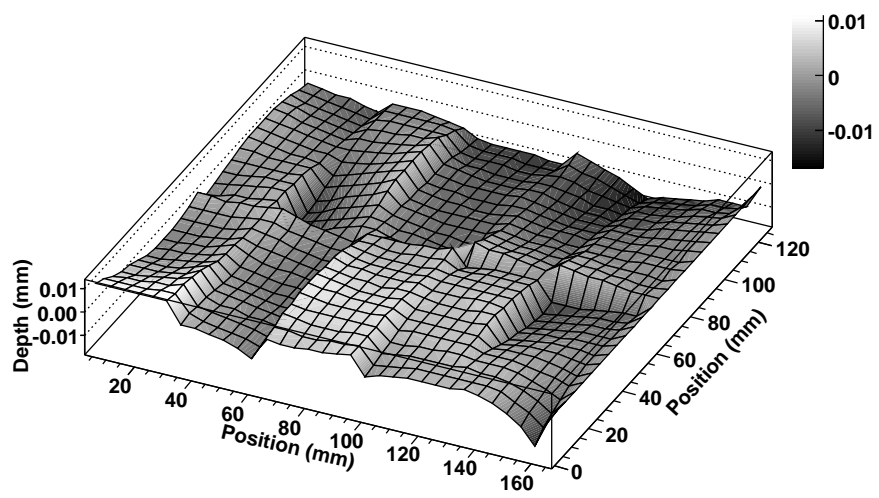


Figure 7: Surface flatness of the CCD array. Grey scale indicates the relative depth of each measurement point. Total 832 points were measured.

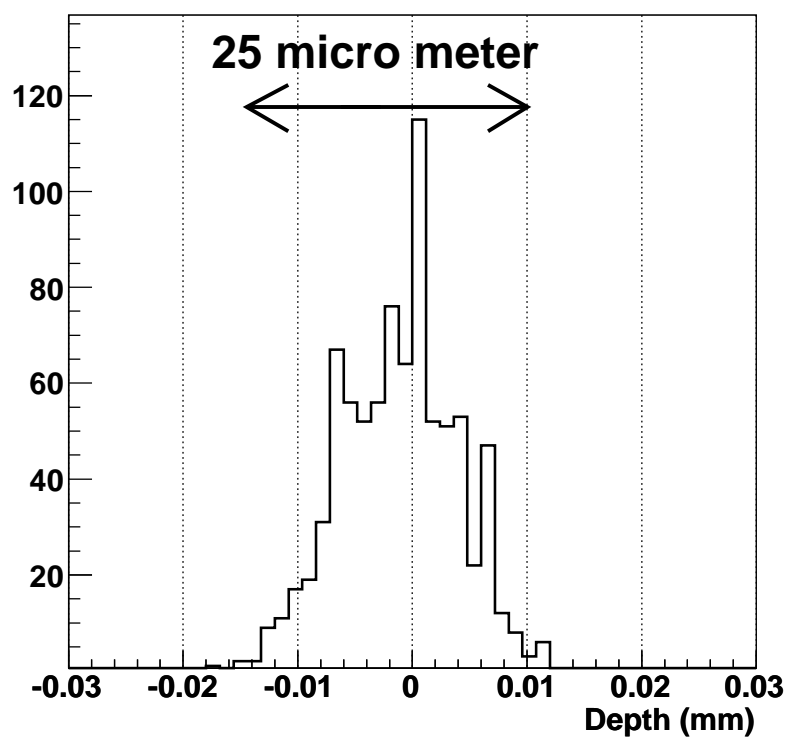


Figure 8: Depth distribution of the Fig.7.

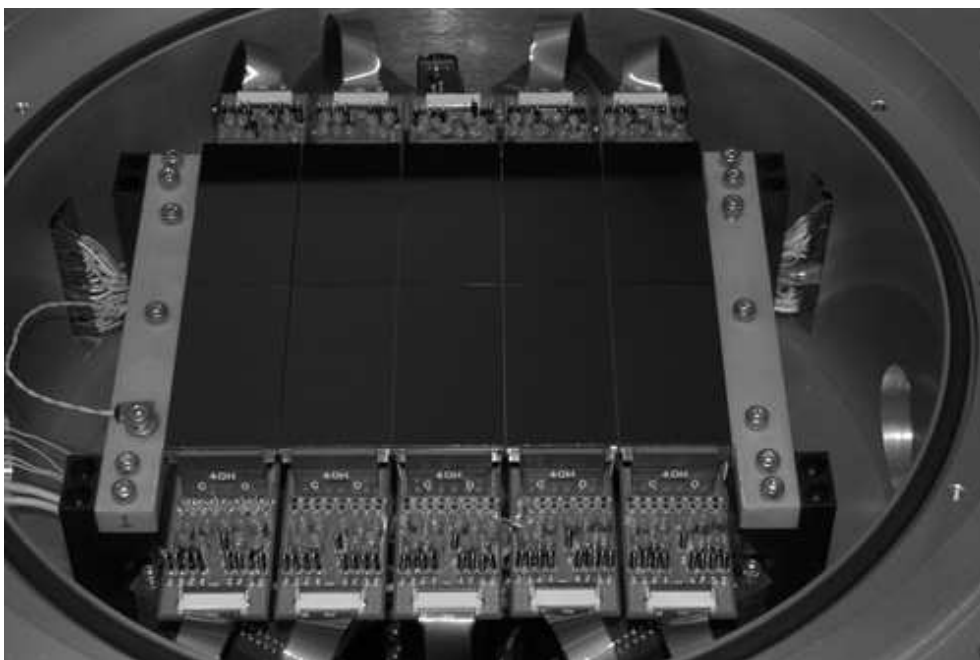


Figure 9: Photo of the ten CCD array mounted on the AlN plate.

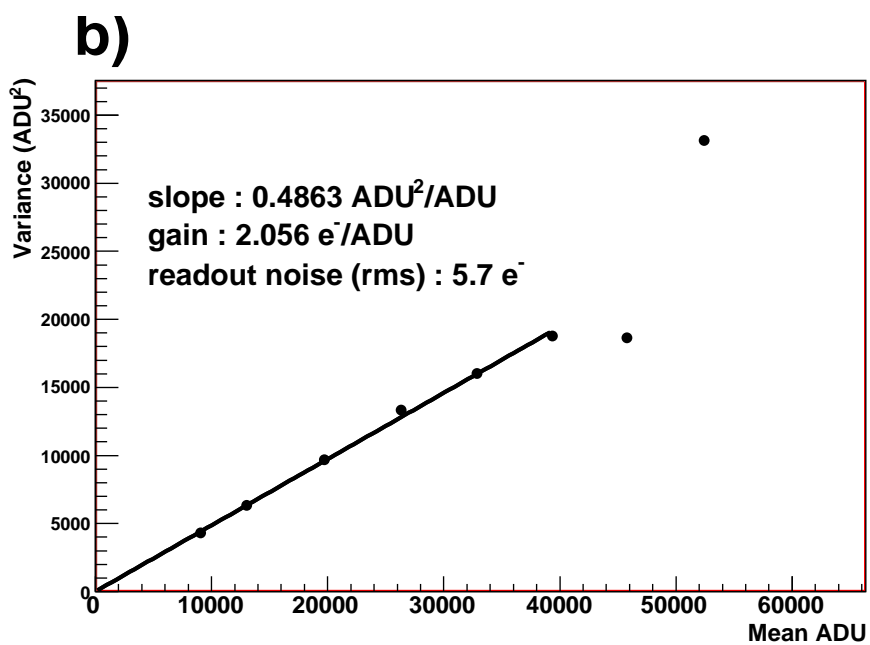
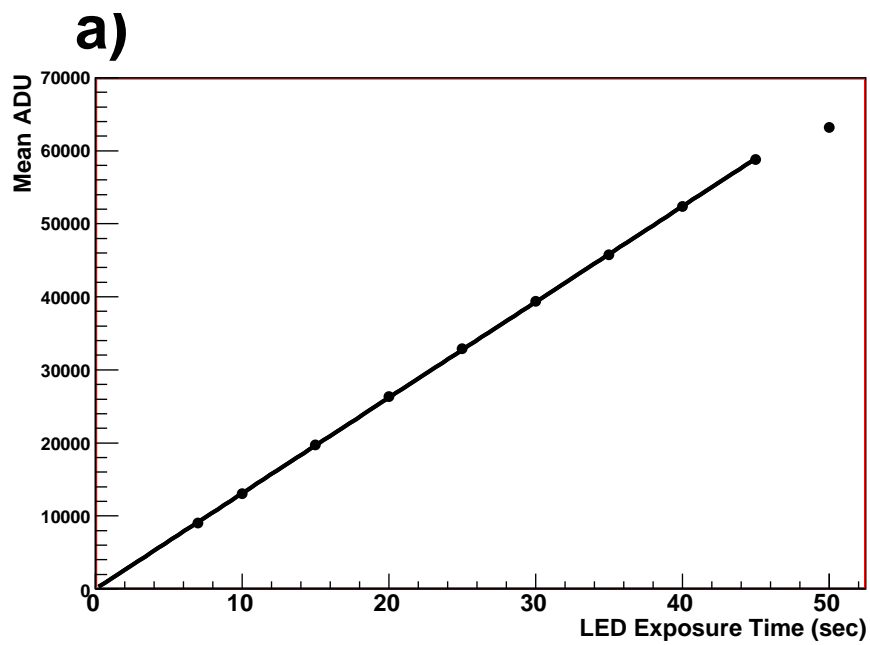


Figure 10: Measurement of the CCD linearity and dynamic range.

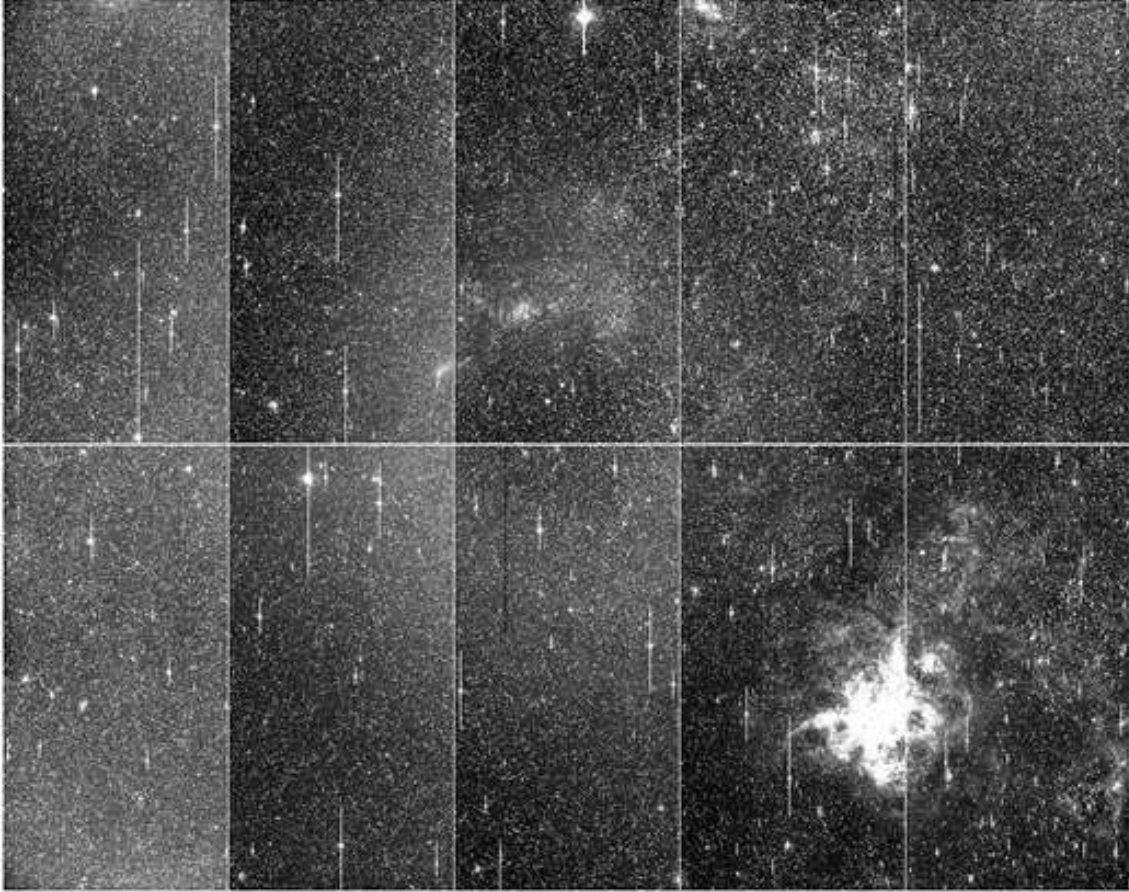


Figure 11: Combined 10 chip image of a part of the Large Magellanic Cloud taken by MOA-cam3. The Tarantula nebula (30 Doradus; $\sim 0.4^\circ$ in diameter) seen in the right bottom corner shows the wide field of the system.